

Analysis of a Clamped Skew Plate under Uniform Loading

C. S. KALE,* S. GOPALACHARYULU,† AND
B. S. RAMACHANDRA RAO‡

Indian Institute of Technology, Bombay, India

Introduction

IN recent years a number of authors have analyzed the bending of a clamped skew plate under uniform loading and still it continues to attract the attention of investigators. Many of the solutions are very approximate. Based on generalized method postulated by Lardy, Mirsky¹ presented the solution which involves considerable algebraic and numerical work. Otta and Hamada² presented the solution for a clamped rhombic plate using strain energy method. Warren³ used a point matching method satisfying the symmetry conditions along the diagonal "exactly" at N discrete points. Morley⁴ derived the solution by reducing the problem to the single membrane boundary value problem. Kennedy⁵ used a simple polynomial form having polar symmetry with a set of three undetermined parameters. He used Galerkin's technique to evaluate those parameters. Iyengar and Srinivas⁶ used a double infinite series of beam functions satisfying the boundary conditions. The unknown constants were determined by satisfying the governing equation.

Although the governing fourth-order differential equation remains the same for a skew plate and a rectangular plate, the solution for the skew plate becomes much more complicated due to its geometry (Fig. 1). The mathematical model of the problem is relatively difficult and explicit solutions are uncommon. In this Note, the eigenfunction expansion method is suggested for the problem. The method owes its originality to Gaydon and Shephard.⁷ The effectiveness of the method over other methods is also indicated.

Statement of the Problem

The governing equation is

$$\frac{\partial^4 w}{\partial x^4} - 4 \cos \alpha \frac{\partial^4 w}{\partial x^3 \partial y} + 2(1 + 2 \cos^2 \alpha) \frac{\partial^4 w}{\partial x^2 \partial y^2} - 4 \cos \alpha \frac{\partial^4 w}{\partial x \partial y^3} + \frac{\partial^4 w}{\partial y^4} = \frac{Q_0 \sin^4 \alpha}{D} \quad (1)$$

where Q_0 is the uniform loading; α is the included angle; and D is the flexural rigidity of the plate. The boundary conditions are

$$w = \partial w / \partial x = 0 \quad \text{at} \quad x = \pm a \quad (2)$$

$$w = \partial w / \partial y = 0 \quad \text{at} \quad y = \pm b \quad (3)$$

Solution

The general solution to Eq. (1) can be written in the form

$$w = w_0 + w_H \quad (4)$$

where w_0 is the particular solution

$$w_0 = (Q_0 \sin^4 \alpha / 24D)(b^2 - y^2)^2 \quad (5)$$

and w_H is the homogeneous solution. The form of the suggested homogeneous solution is

$$w_H = e^{\lambda x} F(y) \quad (6)$$

Substituting Eq. (6) into Eq. (1)

$$\lambda^4 F - 4 \cos \alpha \lambda^3 F' + 2(1 + 2 \cos^2 \alpha) \lambda^2 F'' - 4 \cos \alpha \lambda F''' + F'''' = 0 \quad (7)$$

The boundary conditions given by Eq. (3) modify to

$$F = F' = 0 \quad \text{at} \quad y = \pm b \quad (8)$$

where primes denote differentiation with respect to y . Using the boundary conditions given by Eq. (8) we obtain the solution of Eq. (7) as

$$F_k(y) = (e^{\lambda_k y} \cos \alpha / e^{\lambda_k b} \cos \alpha) B_k \cdot \Phi_k(y) + (e^{\rho_k y} \cos \alpha / e^{\rho_k b} \cos \alpha) C_k \psi_k(y) \quad (9)$$

where

$$\Phi_k(y) = -b \cdot \tan(\lambda_k b \sin \alpha) \cos(\lambda_k y \sin \alpha) + y \cdot \sin(\lambda_k y \sin \alpha) \quad (10)$$

$$\psi_k(y) = -y \cdot \tan(\rho_k b \sin \alpha) \cos(\rho_k y \sin \alpha) + b \cdot \sin(\rho_k y \sin \alpha) \quad (11)$$

λ_k and ρ_k are evaluated from the equations

$$\sin(2\lambda b \sin \alpha) + 2\lambda b \sin \alpha = 0 \quad (12)$$

$$\sin(2\rho b \sin \alpha) - 2\rho b \sin \alpha = 0 \quad (13)$$

B_k and C_k are two unknown sets of complex constants to be determined from the boundary conditions (2).

Taking into consideration the condition of polar symmetry, that is, $w(x, y) = w(-x, -y)$, and $w(x, -y) = w(-x, y)$, we write the complete solution as

$$w = \sum_k B_k \frac{e^{\lambda_k x}}{e^{\lambda_k a}} \frac{e^{\lambda_k y} \cos \alpha}{e^{\lambda_k b} \cos \alpha} \Phi_k(y) + \sum_k B_k \frac{e^{-\lambda_k x}}{e^{\lambda_k a}} \cdot \frac{e^{-\lambda_k y} \cos \alpha}{e^{\lambda_k b} \cos \alpha} \Phi_k(y) + \sum_k C_k \frac{e^{\rho_k x}}{e^{\rho_k a}} \cdot \frac{e^{\rho_k y} \cos \alpha}{e^{\rho_k b} \cos \alpha} \psi_k(y) - \sum_k C_k \frac{e^{-\rho_k x}}{e^{\rho_k a}} \cdot \frac{e^{-\rho_k y} \cos \alpha}{e^{\rho_k b} \cos \alpha} \psi_k(y) + \text{the conjugate} + \frac{Q_0 \sin^4 \alpha}{24D} (b^2 - y^2)^2 \quad (14)$$

Unfortunately the solutions $F_k(y)$ are not an orthogonal set. However, this difficulty is overcome by expanding them in terms of clamped beam functions. The advantage of the clamped beam functions is that they are real functions which simplify evaluation of coefficients. Secondly, since they satisfy the same fourth-order differential equation with the same four boundary conditions as do the original function, they give rise to expansion which is considerably more convergent than would have been obtained with the Fourier series. Therefore, expanding

$$\frac{\cosh(\lambda_k y \cos \alpha)}{e^{\lambda_k b} \cos \alpha} \Phi_k(y) = \sum_m b_{1km} Y_m \quad (15)$$

$$\frac{\sinh(\gamma_k y \cos \alpha)}{e^{\lambda_k b} \cos \alpha} \Phi_k(y) = \sum_m b_{2km} Z_m \quad (16)$$

$$\frac{\sinh(\rho_k y \cos \alpha)}{e^{\rho_k b} \cos \alpha} \psi_k(y) = \sum_m c_{1km} Y_m \quad (17)$$

$$\frac{\cosh(\rho_k y \cos \alpha)}{e^{\rho_k b} \cos \alpha} \psi_k(y) = \sum_m c_{2km} Z_m \quad (18)$$

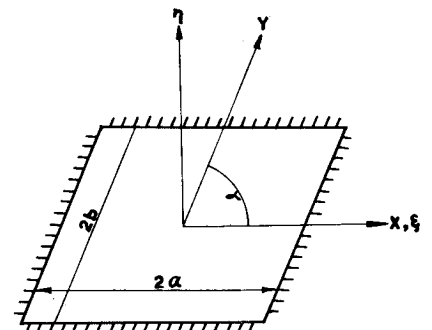
$$\frac{Q_0 \sin^4 \alpha}{24D} (b^2 - y^2)^2 = \sum_m R_m Y_m \quad (19)$$

where Y_m and Z_m are even and odd beam functions

$$Y_m = \frac{1}{(2b)^{1/2}} \left[\frac{\cos(\mu_m y/b)}{\cos \mu_m} - \frac{\cosh(\mu_m y/b)}{\cosh \mu_m} \right] \quad (20)$$

$$Z_m = \frac{1}{(2b)^{1/2}} \left[\frac{\sin(v_m y/b)}{\sin v_m} - \frac{\sinh(v_m y/b)}{\sinh v_m} \right] \quad (21)$$

Fig. 1 Clamped skew plate under uniform loading.



Received August 11, 1971.

* Graduate Student, Mechanical Engineering Department.

† Assistance Professor, Department of Mechanical Engineering.

‡ Lecturer, Department of Mathematics.

μ_m and v_m can be obtained from

$$\tan \mu + \tanh \mu = 0$$

and

$$\tan v - \tanh v = 0, \text{ respectively} \quad (22)$$

The constants b_{1kn} , c_{1kn} , R_n can be obtained by multiplying both sides of the Eqs. (16, 19 and 20) by Y_n and integrating between the limits $-b$ to $+b$. Similarly, b_{2kn} and c_{2kn} are obtained by multiplying both sides of the Eqs. (17) and (18) by Z_n and integrating between $-b$ to $+b$.

The form of the solution w changes to

$$w = \sum_k \sum_n 2B_k \frac{\cosh(\lambda_k y)}{e^{\lambda_k a}} b_{1kn} Y_n + \sum_k \sum_n 2B_k \frac{\sinh(\lambda_k y)}{e^{\lambda_k a}} b_{2kn} Z_n + \sum_k \sum_n 2C_k \frac{\cosh(\rho_k y)}{e^{\rho_k a}} c_{1kn} Y_n + \sum_k \sum_n 2C_k \frac{\sinh(\rho_k y)}{e^{\rho_k a}} c_{2kn} Z_n + \text{the conjugate} + \sum_n R_n Y_n \quad (23)$$

Using the boundary conditions (2), we obtain four simultaneous equations and two unknown complex constants namely

$$\sum_k B_k \frac{\cosh(\lambda_k a)}{e^{\lambda_k a}} b_{1kn} + \sum_k C_k \frac{\cosh(\rho_k a)}{e^{\rho_k a}} c_{1kn} = -\frac{R_n}{4} \quad (24)$$

$$\sum_k B_k \frac{\sinh(\lambda_k a)}{e^{\lambda_k a}} b_{2kn} + \sum_k C_k \frac{\sinh(\rho_k a)}{e^{\rho_k a}} c_{2kn} = 0 \quad (25)$$

$$\sum_k B_k \lambda_k \frac{\sinh(\lambda_k a)}{e^{\lambda_k a}} b_{1kn} + \sum_k C_k \rho_k \frac{\sinh(\rho_k a)}{e^{\rho_k a}} c_{1kn} = 0 \quad (26)$$

$$\sum_k B_k \lambda_k \frac{\cosh(\lambda_k a)}{e^{\lambda_k a}} b_{2kn} + \sum_k C_k \rho_k \frac{\cosh(\rho_k a)}{e^{\rho_k a}} c_{2kn} = 0 \quad (27)$$

from which we can evaluate the constants B_k and C_k .

Numerical results

Numerical results are obtained for the deflection and maximum principle bending moments at the center using three-

term series and five-term series (the results are presented in Table 1).

$$\text{deflection coefficients} = w_{\max} D/Q_0 a^4 \times 10^2$$

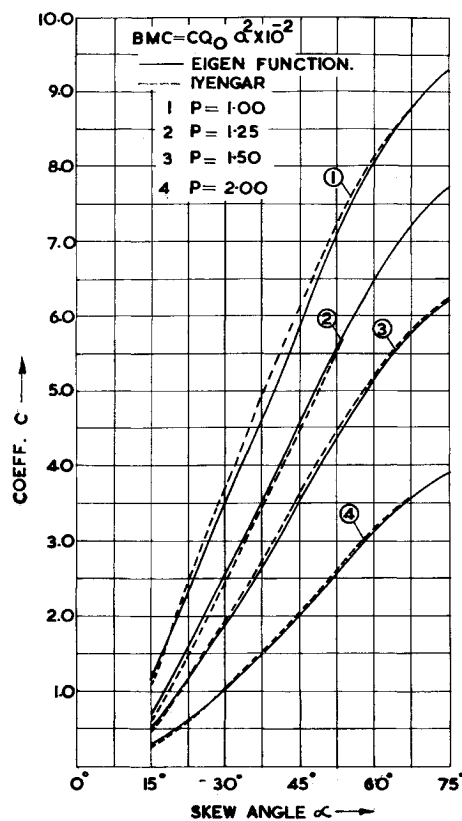


Fig. 2 Maximum bending moment at the center.

Table 1 Deflection coefficients^a

Skew angle 90°-α	P = 1.0			P = 1.25		
	Iyengar	Kennedy	Our method	Iyengar	Kennedy	Our method
15	1.79680 ^b	1.79296	1.79766 ^c 1.79675 ^d	1.05744	1.05504	1.05760 1.05732
30	1.22992	1.18112	1.23146 1.23083	0.71824	0.69600	0.72021 0.71874
45	0.60176	0.50800	0.61147 0.61242	0.34592	0.30096	0.35217 0.34872
60	0.17168	0.12000	0.19856 0.19502	0.09568	0.07168	0.10114 0.09989
75	0.01443	0.00826	0.01879 0.01870	0.00755	0.00494	0.00767 0.00767
Skew angle 90°-α	P = 1.5			P = 2.0		
	Iyengar	Kennedy	Our method	Iyengar	Kennedy	Our method
15	0.61200	0.61104	0.61206 0.61197	0.22176	0.22096	0.22158 0.22157
30	0.40976	0.40496	0.41040 0.41003	0.14496	0.14704	0.14496 0.14494
45	0.19184	0.17696	0.19353 0.19257	0.06512	0.06560	0.06525 0.06520
60	0.05056	0.04256	0.05116 0.05112	0.01632	0.01616	0.01633 0.01633
75	0.003692	0.00296	0.003692 0.003692	0.001168	0.001136	0.001168 0.001168

^a P = a/b.

^b Truncation of the series on 50th term.

^c Truncation of the series on 3rd term.

^d Truncation of the series on 5th term.

Discussions

The deflection and bending moment at the center for the skew plate with aspect ratio equal to 1.0, 1.25, 1.5, and 2.0 and for included angles 75°, 60°, 45°, 30°, and 15° are calculated. The convergence of deflections and bending moments have been studied, by taking 3 and 5 terms. They are compared with available results. It should be noted that Iyengar and Srinivas obtained the values with 50 term series.

Deflections are given in Table 1. The values given by Kennedy are less than those here; and for large skew angles the difference is large. The values agree satisfactorily with those given by Iyengar and Srinivas.

Maximum principle bending moment coefficients at the center are compared with Iyengar's values in the graph (Fig. 2), Poisson's ratio is $\frac{1}{3}$.

As may be observed from the Table 1 that, the effect of increasing skew angle is to reduce the deflection and the effect of skew on maximum deflection decreases with the increasing aspect ratio.

References

- 1 Mirsky, I., "The Deflection of a Thin Flat Parallelogram Plate under Pressure," ARL Rept. SM 175, 1951, Dept. of Supply, Australia.
- 2 Otta, T. and Hamada, N., "Statistical Deflection of a Rhomboidal Plate with Clamped Edges Subjected to Uniformly Distributed Pressure," *Bulletin of Japan Society of Mechanical Engineers*, Vol. 6, No. 21, 1963, pp. 1-7.
- 3 Warren, W. E., "Bending of Rhombic Plates," *AIAA Journal*, Vol. 2, No. 1, Jan. 1964, pp. 166-168.
- 4 Morley, L. S. D., "Solution for Bending of a Clamped Rectangular Plate under Uniform Normal Load," *Quarterly Journal of Mechanics and Applied Mathematics*, Vol. 16, 1963, pp. 109-114.
- 5 Kennedy, J. B., "On Bending of a Clamped Skew Plate under Uniform Pressure," *Journal of the Royal Aeronautical Society*, Vol. 69, 1965, pp. 352-355.
- 6 Iyengar, K. T. S. R. and Srinivas, R. S., "Clamped Skew Plates under Uniform Normal Loading," *Journal of the Royal Aeronautical Society*, Vol. 71, 1967, pp. 139-140.
- 7 Gaydon, F. A. and Shephard, W. M., "Generalized Plane Stress in a Semi-Infinite Strip under Arbitrary 'End Load'," *Proceedings of the Royal Society of London*, Vol. 281, 1964, pp. 184-206.

Position Determination from Star-Gravity Measurements

R. H. KIDD* AND J. N. DASHIELL†
TRW Systems Group, Houston, Texas

AND

T. J. BLUCKER‡
NASA Manned Spacecraft Center, Houston, Texas

Introduction

THIS paper presents a description of a computational technique to determine the position of an observer on the surface of a planet from measurements of the unit gravity direction and star line of sight directions. The uncertainty in the direction of the gravitational potential of the planet is shown to determine

Presented as Paper 71-900 at the AIAA Guidance, Control and Flight Mechanics Conference, Hempstead, N.Y., August 16-18, 1971; submitted August 19, 1971; revision received December 27, 1971.

Index category: Spacecraft Navigation, Guidance, and Flight Path Control Systems.

* Staff Engineer, Systems Analysis and Software Department, TRW Houston Operations.

† Member of Technical Staff, Systems Analysis and Software Department, TRW Houston Operations.

‡ Aerospace Technologist, Mission Planning and Analysis Division.

the limiting accuracy of the estimator. Numerical results are presented to illustrate the convergence properties of the filter and to compare the filter solutions for the successful Apollo landing missions with other solutions for the landing sites.

For the Apollo missions, the selenographic position coordinates for the Lunar Module have been determined by a variety of methods. Most of these solutions are obtained relative to the position of the orbiting Command Module. Experience has shown that orbital position uncertainties, rather than the errors in the measurement devices, limit the accuracy of these LM position solutions.

The methods to determine Lunar Module (or landmark) position, which are functions of the orbiter position, are a) Command Module optical line of sight tracking, b) Lunar Module rendezvous radar tracking (angles, range and range rate) of the Command Module from the lunar surface, c) lunar mapping (photography from Apollo and Lunar Orbiter missions) confirmed by crew visual observations, and, d) the latitude, longitude and radius of a position vector near the time of Lunar Module powered descent initiation is used with the measured incremental change from these three quantities down to the surface. The increments are determined by the primary Lunar Module guidance system, by the auxiliary guidance system, and by a ground based high-speed computer recursive filter.

The object of this paper is to present a filter technique for position determination, which is independent of an orbiter's position uncertainties, that processes measured star line of sight directions and measured gravity directions. A weighted least-squares filter is formulated and its accuracy is shown to be limited by the uncertainties of the gravitational potential model. The convergence properties of this filter are shown to be excellent.

The position solutions from this star-gravity method for three Apollo missions are presented and compared to the best estimates of the actual landing site locations. These comparisons show that the solution accuracy of this filter is comparable to the methods discussed previously.

Filter Development

The use of star vector and gravity vector measurements to determine position can be illustrated by considering the deterministic problem when only two measurements are available. These measurements are shown in Fig. 1, where $\mathbf{r}^T = [\cos \phi \cos \lambda, \cos \phi \sin \lambda, \sin \phi]$ is the position vector, ϕ is latitude, λ is longitude, α_i is the angle between the position vector and the i th star vector, and the superscript T denotes the transpose operation.

If the measurements are the cosine of the angle between the star vector and the measured gravity vector, and the gravity vector is assumed to be along negative \mathbf{r} , then the measurements become

$$m_i = -\cos \alpha_i$$

The dot product of the unit gravity vector (as a function of ϕ and λ) with the known unit star vector yields the two equations

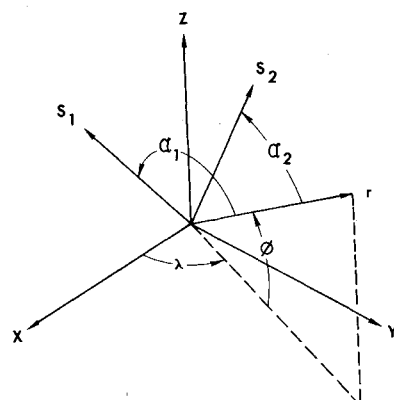


Fig. 1 Position determination with two star-gravity measurements.